alternating field for a long time, U_{th} increases some-
what. Apparently this is due to some smoothing out of
the distortion and to a corresponding diminution of the
amount of the space charge. At high frequencies, the
space charge lags in phase behind the applied voltage
in the direction perpendicular to the field. Therefore
with increase of the frequency of the external field, U_{th}
increases.

While having a number of common features, EHD
instability in the smectic A phase differs from its
analog in the nematic state. First, motion of a smec-
tic liquid at once acquires turbulent character, and
destruction of the layered structure occurs without
the rotary flow that is usually observed in the form of
nematic Williams domains. Second, in contrast to in-
stability in NLC, U_{th} in SLC depends on the thickness
d of the sample (Fig. 6). There is a relation of direct
proportionality between U_{th} and d, in confirmation of
theoretical calculations (see formula (9) of Ref. 4). At
the same time, the threshold of the conformal-homo-
tropic transition is proportional to $\sqrt{d}$ (Fig. 6, Curve 5).

[1] A. Rapini, J. Phys. (Paris) 33, 237 (1972).
[2] O. Parodi, Solid State Commun. 11, 1503 (1972).
[3] M. Goscianski, L. Leger, and A. Mircea-Roussel, J. Phys. (Paris) Lett. 36, L-313 (1975).
[4] J. A. Geurst and W. A. Goosens, Phys. Lett. 41A, 369 (1972).
[5] V. N. Chirkov, D. F. Aliev, and A. Kh. Zeĭnally, Pis'ma Zh. Tekh. Fiz. 3, 1016 (1977) [Sov. Tech. Phys. Lett. 3, 417 (1977)].
[6] E. F. Carr, Phys. Rev. Lett. 24, 807 (1970).
[7] G. Heppke, W. E. Montserrat Benavent, and F. Schneider, Z. Naturforsch. 29a, 728 (1974).
[8] K. Yoshino, K. Yamashiro, and Y. Inuishi, Jap. J. Appl. Phys. 14, 216 (1975).
[9] K. Yoshino, N. Tanaka, and Y. Inuishi, Jap. J. Appl. Phys. 15, 735 (1976).
[10] E. F. Carr, Mol Cryst. Liq. Cryst. 7, 253 (1969).
[11] W. Helfrich, J. Chem. Phys. 51, 4092 (1969).
[12] E. Dubois-Violette, P. G. de Gennes, and O. Parodi, J. Phys. (Paris) 32, 305 (1971).

Translated by W. F. Brown, Jr.

Variation of the connectivity of the electron constant-energy surface in Bi under pressure

N. B. Brandt, V. V. Moshchalkov, and S. M. Chudinov

Moscow State University
(Submitted 2 December 1977)
Zh. Eksp. Teor. Fiz. 74, 1829–1844 (May 1978)

The Shubnikov–de Haas (SdH) effect in single-crystal samples of Bi and Bi–Te alloys is investigated at
hydrostatic pressures, p, of up to 20 kbar in magnetic fields of up to 60 kOe at helium temperatures. It
is found that hydrostatic pressure induces a transition of the electron constant-energy surface (ECES)
from a quasi-ellipsoidal to a dumbbell-like shape and then to a doubly connected surface. A magnetic-field-
induced change in the connectivity of the ECES is observed in the region of pressures where the cross
section of the neck of the dumbbell becomes sufficiently small. The shape of the ECES at different
pressures p is established from the angular dependences of the SdH-oscillation frequencies. The obtained
pressure dependences of the extremal cross sections, S, of the ECES are discussed on the basis of the
McClure band spectrum model for materials of the Bi type. The computed $S(p)$ functions agree with the
experimental functions if it is assumed that the spectrum at the L point of the Brillouin zone is inverted
and $\epsilon_{gL} \sim -7$ meV. It is found that the parameter ratio $Q_{22}{}^2/\alpha_v < 0.0005$ a.u. in the McClure model.

INTRODUCTION

The band structure and the Fermi surface (FS) of the
current carriers in Bi have been investigated in a large
number of experiments by different methods (compre-
hensive lists of references on this question are given in
Fal'kovskiĭ's[1] and Édel'man's[2] review articles). The
data obtained in the investigations on Bi were up until
very recently interpreted on the basis of two different
band-spectrum theories: the Lax theory[3] and the Ab-
rikosov-Fal'kovskiĭ (AF)[4,5] theory. It follows from
Lax's two-band model that the electron constant-energy
surfaces (ECES) in Bi are ellipsoidal, while the electron

and hole spectrum at the L point of the Brillouin zone is
a mirror spectrum and is the same whether the spec-
trum at the L point is inverted $(\varepsilon_{gL} \equiv \varepsilon(L_a) - \varepsilon(L_s) < 0$; the
bottom of the conduction band is formed by the L_s term,
while the bottom of the valence band is formed by the L_a
term, it being then possible for saddle points to exist in
the spectrum) or direct $(\varepsilon_{gL} > 0$; the spectrum cannot
contain saddle points).

In principle, the Lax model cannot explain the experi-
mentally established deviation[6,7] of the ECES in Bi
from the ellipsoidal shape. The AF model satisfactorily
describes the angular dependences of the cyclotron

masses[8] and the quantum-oscillation periods.[6] But it is in this case impossible to correlate the data computed on the basis of the AF model with the experimental values of the cyclotron masses in the central orbits and at the reference points,[7] the quantum-oscillation periods,[7,9] and the Fermi momenta[10] to within, on the average, something smaller than 8%,[11] which is significantly lower than the experimental error in the determination of these quantities. The fundamental difference between the AF theory and the Lax model consists in the dependence of the energy ε on the quasimomentum $\mathbf{k}$ when $\mathbf{k}$ is directed along the direction of elongation of the ECES. According to the Lax model, the energy ε depends linearly on $\mathbf{k}$ in all directions. In the AF model, however, there is no linear term in $\mathbf{k}$ for the direction along the long ECES axis:

$$(\varepsilon_F - \tfrac{1}{2}\varepsilon_{gL} - k_y^2/2M_1)(\varepsilon_F + \tfrac{1}{2}\varepsilon_{gL} + k_y^2/2M_2) = v_x^2 k_x^2 + v_z^2 k_z^2. \tag{1}$$

Here k_x, k_y, and k_z are the wave-vector components; M_1, M_2, v_x, and v_z are parameters of the spectrum, and ε_F is the Fermi energy, measured from the middle of the gap ε_{gL}.

According to the AF model, for $\varepsilon_{gL} < 0$ two saddle points, corresponding to the energies $\pm\tfrac{1}{2}\varepsilon_{gL}$, exist in the spectrum at the points $k_y = 0$, the conduction band overlaps the valence band, and the spectrum is degenerate at the points

$$\pm k_{y0} = [-2\varepsilon_{gL} M_1 M_2/(M_1 + M_2)]^{1/2}$$

(the electron and hole terms $\varepsilon(k_y)$ intersect).

McClure[12] has shown that the linear term also appears in calculations based on deformation theory if the spin-orbit interaction, which mixes the various spin states, is taken into account. Calculations carried out by the method of pseudopotentials[13,14] and experimental data[15,16] indicate that the linear term is as important as the quadratic—in k—terms introduced by Cohen[17] and Abrikosov and Fal'kovskiĭ.[4] The dispersion law obtained by McClure[12] can be written as follows

$$(\varepsilon - \tfrac{1}{2}\varepsilon_{gL} - K_1)(\varepsilon + \tfrac{1}{2}\varepsilon_{gL} - K_0) = Q_{11} k_x^2 + Q_{22} k_y^2 + Q_{33} k_z^2,$$

$$K_1 = \tfrac{1}{2}\alpha_c k_y^2, \quad K_0 = -\tfrac{1}{2}\alpha_v k_y^2, \quad Q_{22} \neq 0. \tag{2}$$

Here ε_{gL} is the gap at L, the energy ε is measured from the middle of the gap, k_x is parallel to the binary axis, k_z makes an angle of 6° with the trigonal axis, k_y is perpendicular to k_x and k_z and directed along the long ECES axis. In the AF theory

$$K_0 = -k_y^2/2M_2, \quad K_1 = k_y^2/2M_1, \quad Q_{22} = 0,$$

while in the Lax model

$$K_0 = K_1 = 0, \quad Q_{22} \neq 0.$$

For $Q_{22} \neq 0$ in the expression (2) the degeneracy at the points $\pm k_{y0}$ [see (1)] is removed. In the case of a negative gap (i.e., for $\varepsilon_{gL} < 0$) the saddle point in the conduction (valence) band is preserved also for the dispersion law (2) if

$$Q_{22}^2/\alpha_v < \tfrac{1}{2}|\varepsilon_{gL}| \quad (Q_{22}^2/\alpha_c < \tfrac{1}{2}|\varepsilon_{gL}|). \tag{3}$$

When the inverses of the inequalities (3) are fulfilled, there are no saddle points and the inverted spectrum differs from the direct spectrum only in having a flatter band bottom. Using (2), McClure[12] achieved an agreement between theory and the experimental data that is better than the agreement that has been achieved with other models.[3-5] However, in this case it turned out to be impossible to obtain a unique set of parameters, ε, ε_{gL}, Q_{11}, Q_{22}, Q_{33}, α_c, and α_v, from the experimental data, since only quantities found for an energy fixed at the Fermi level—quantities which are not very sensitive to the structure of the bottom of the band—were used.

The most reliable information about the structure of the spectrum $\varepsilon(k)$ at the L point of the Brillouin zone can, in our view, be obtained through the variation of the ratio of the Fermi energy ε_F to the magnitude of the gap ε_{gL}. One way of varying the ratio $\varepsilon_F/\varepsilon_{gL}$ is to alloy bismuth with antimony. The extrapolation to $x = 0$ of the dependence of the gap at L in the alloys $Bi_{1-x}Sb_x$ on the concentration x gives grounds to suppose that the spectrum at L in Bi is inverted and that $\varepsilon_{gL} = -(5 \pm 2)$ meV.[18] The behavior of the gap ε_{gL} in Bi in a strong magnetic field, computed on the basis of the analysis of the shape of the magnetooptical-transition lines[16] is similar to the variation in an H field of the gap ε_{gL} in the semiconducting alloys $Bi_{1-x}Sb_x$, which have an inverted spectrum ($p > p_{inv}$, $\varepsilon(L_S) > \varepsilon(L_a)$),[18] which also indicates the inverse disposition of the L_S and L_a terms in Bi. The doping of Bi with donor (Te, Se) or acceptor (Pb, Sn) impurities also changes the ratio $\varepsilon_F/\varepsilon_{gL}$. Measurements performed on doped alloys yield the following value for ε_{gL}: $\varepsilon_{gL} = -(4 \pm 4)$ meV[19] and $|\varepsilon_{gL}| < 15$ meV.[20]

Investigations of the $Bi_{1-x}Sb_x$ alloys have shown that, under pressure, the L_S term always moves upwards relative to the L_a term with a velocity $\partial|\varepsilon_{gL}|/\partial p = 2.5 \pm 0.2$ meV/kbar. Thus, it is possible to increase under the action of hydrostatic pressure the value of $|\varepsilon_{gL}|$ to such an extent that it becomes comparable to, or exceeds, the Fermi energy. In this case, for $|\varepsilon_{gL}| > 2Q_{22}^2/\alpha_v$ the invertedness of the spectrum in Bi should manifest itself in a qualitative change in the shape of the ECES; to begin with the quasiellipsoidal ECES goes over into a dumbbell-like shape and then into a doubly-connected surface. The possibility of the appearance of a dumbbell-shaped or a doubly-connected ECES in materials of the Bi type was first pointed out by Abrikosov.[5] If $2Q_{22}^2/\alpha_v > |\varepsilon_{gL}|$, then a qualitative change in the ECES does not occur: the shrinking ECES will all the time remain quasiellipsoidal.

Thus, the investigation of the ECES shape in Bi under pressure allows us to obtain additional information about the sign of the gap ε_{gL} and about the magnitude of the parameter Q_{22} in Bi. The effect of hydrostatic pressure on the shape of the electron and hole FS in Bi has been investigated in a number of papers.[21-25] It has been observed that the carrier concentration decreases with pressure and that the small cross section of the hole ellipsoid and the near-minimal cross section of the ECES in the case when the field is oriented along the two-fold axis monotonically decrease with pressure p. The dependence of the large cross section of the ECES on p

could not be measured in these investigations. The decrease of the carrier concentration with increasing p gives rise to considerable difficulties in the observation of the Shubnikov-de Haas (SdH) oscillations starting from pressures ~10 kbar.

In view of this, more promising for the study of the effect of pressure on the shape of the ECES in Bi are samples of Bi slightly doped with Te (up to ~0.01 at.% Te). Doping with Te increases with electron concentration and, consequently, the number of observable periods in the SdH oscillations in the high-pressure region, which significantly increases the accuracy of determination of the oscillation frequencies. Furthermore, doping with Te increases the contribution from the oscillations corresponding to the large ECES cross sections,[26] which allowed the first observation of the pressure dependence of the frequency of these oscillations in Bi samples doped with Te in the region of sufficiently high pressures.

In the present paper we present the results of an investigation of the SdH oscillations in single-crystal samples of Bi and Bi-Te alloys at helium temperatures and hydrostatic pressures of up to 20 kbar in magnetic fields of up to 60 kOe. The pressure dependences of the oscillation frequencies in the case when the field is oriented along the principal crystallographic axes of the single-crystal samples, as well as the angular dependences of the oscillation frequencies when the field is rotated in the basal plane at different fixed pressures, have been studied.

MEASUREMENT PROCEDURE. SAMPLES

Hydrostatic pressures of up to 20 kbar were produced with the aid of a pressure booster.[27] As the pressure-transmitting medium we used a dehydrated mixture of 50% kerosene and 50% transformer oil. The magnitude of the pressure was measured at liquid-helium temperatures by a noncontact method[28] involving the measurement of the shift of the critical temperature of the transition into the superconducting state of a tin transducer located in the pressure-booster channel beside the sample. The pressure booster was located either in the inner channel of a superconducting Helmholtz system producing magnetic fields of up to 33 kOe directed perpendicularly to the pressure-booster channel, or inside a superconducting solenoid producing a field of maximum intensity 60 kOe directed along the channel. The samples, which were of rectangular shape (~0.5 × 0.5 × 1.8 mm), were cut out by the electric-spark method from single-crystal slabs of Bi-Te alloys and Bi along the trigonal, binary, or bisector axis. Four Bi-Te alloys with electron concentrations n_e ~ 3.2, 4.0, 4.4, and 4.9 × 10¹⁷ cm⁻³ were investigated. The Bi-Te alloys were kindly made available to us A. D. Belaya (A. A. Baĭkov Institute of Metallurgy).

The SdH oscillations were automatically recorded on an X-Y recorder, using the standard modulation technique, and processed by the Fourier-analysis method on a computer.[29] From the peaks of the spectral-density curves $I(\omega)$ we determined the oscillation-frequen-

cy components ω_i to within 5%. When $H \| C_2$ the oscillations corresponding to the large ECES cross sections and the oscillations when $H \| C_3$ were single-frequency curves. The periods of the oscillaions in this case were determined directly from the dependence of the arbitrary quantum number of the oscillation extrema on the inverse field $1/H$.

VARIATION OF THE SHAPE OF THE ECES UNDER PRESSURE

Near-minimal ECES cross sections were measured in all the investigated Bi-Te-alloy and Bi samples at atmospheric pressure in a field H directed along the binary (C_2) axis. The cyclotron masses m_c^e were determined for the same orientation of H from the temperature dependence of the oscillation amplitudes $\rho_\perp(H)$. From the $\partial\rho/\partial H = f(1/H)$ curves measured in a field $H \| C_3$ we found the minimal hole-FS cross sections S_{min}^h, from which we can compute the relative shift, $\Delta\varepsilon_F$, of the Fermi level, as is done in Ref. 20. The dependence of the square of the cyclotron mass, $(m_c^e)^2$, on the extremal cross section S_{bin}, as well as of S_{bin} on the quantity ε_F^2 computed from the value of ε_F in Bi ($\varepsilon_{FBi} = 33.7$ meV[15,16]) and the shift $\Delta\varepsilon_F(\varepsilon_F = \varepsilon_{FBi} + \Delta\varepsilon_F)$ are in good agreement with the dependences computed from the formulas

$$S_{bin} = \frac{2}{\sqrt{3}}\frac{\pi}{Q_{11}Q_{33}}\left(\varepsilon_F^2 - \frac{\varepsilon_{gL}^2}{4}\right), \qquad m_{c\,bin} = \frac{2}{\sqrt{3}}\frac{\pi}{Q_{11}Q_{33}}\varepsilon_F \qquad (4)$$

(derived from (2)) with the parameters $\varepsilon_{gL} = -7$ meV, $Q_{11} = 0.435$, $Q_{22} = 0.015$, $Q_{33} = 0.327$, $\alpha_c = 1.3$, and $\alpha_v = 1.53$. The good agreement between the calculated and experimental data confirms the applicability of the rigid-band scheme[30,20] for Bi-Te alloys with Te concentrations of not less than 0.01 at.%, which also agrees with the results obtained by Cucka and Barrett[31] in an x-ray structural investigation of these alloys with Te concentrations of up to 0.2 at.%: the lattic parameters for the Bi-Te alloys are the same as for Bi. Therefore, the introduction of a small quantity of Te into Bi does not change the dispersion law for Bi; it only increases the electron concentration, so that the data obtained for the Bi-Te alloys characterize the dispersion law, $\varepsilon(k)$, for Bi.

In the superconducting Helmholtz system an investigation of the effect of pressure on the SdH oscillations from the ECES cross sections close to S_{min} was carried out on samples located along the pressure-booster channel. The orientation of the axes was determined to within ±0.5° from the symmetry of the oscillations from the large ECES cross sections. The $\partial\rho/\partial H = f(1/H)$ curves for H fields oriented along the various equivalent (binary or bisector) directions always coincided with each other. Therefore, everywhere we present the curves measured in an H field parallel to one of the equivalent axes.

In Fig. 1 we show SdH oscillations, characteristic of all the Bi-Te alloys and pure Bi, at different pressures p for an H field directed along the bisectrix (C_1) axis. Up to pressures ~5 kbar the spectral composition of these oscillations is the same as at atmospheric pres-
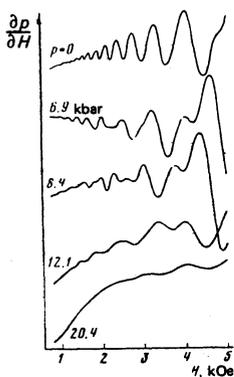
FIG. 1. Oscillations in $\partial\rho/\partial H$ in a magnetic field directed along the bisectrix (C_1) axis in a Bi-Te alloy $(n_e = 4.9 \times 10^{17}\text{cm}^{-3})$ at different pressures.

sure. For $H\|C_2$ the $\partial\rho/\partial H = f(1/H)$ curves have a monochromatic spectrum corresponding to two equal cross sections of the electron quasiellipsoids. For $H\|C_1$ the oscillations are a superposition of two frequencies: the first frequency is the oscillation from the S_{min} of the ECES and the second, which is twice higher than the first, is the oscillation frequency from two other ECES. In the ~5—13 kbar pressure range the spectrum of the oscillations is appreciably complicated: the oscillations in $H\|C_1$ contain four different frequencies: $\omega_1 < \omega_2 < \omega_3 < \omega_4$ with $2\omega_1 \approx \omega_3$ and $2\omega_2 \approx \omega_4$, while the oscillations for $H\|C_2$ contain two frequencies. In the region of pressures $p \gtrsim 13$ kbar the $\partial\rho/\partial H = f(1/H)$ curves again represent a superposition of two frequencies, ω_1 and ω_2 ($\omega_2 \approx 2\omega_1$), when $H\|C_1$ and a monochromatic frequency when $H\|C_2$. The pressure dependences of the extremal cross sections S pertaining to the same ECES are shown in Fig. 2 ($H\|C_1$) and Fig. 3b.

The angular dependences of the oscillations were measured for several fixed pressures as the field H was rotated in the basal plane (Fig. 4). Figure 5 shows computer-separated extremal cross sections ($p = 8.4$ kbar).

The dependence of S on φ for a highly anisotropic

FIG. 3. a) Dependence on pressure of the frequency, Ω^e_{max}, of the oscillations from the maximal cross section of the ECES in a Bi-Te alloy $(n_e = 4.9 \times 10^{17}\text{cm}^{-3})$ in $H\|C_2$. The solid curve is the theoretical Ω^e_{max} curve, computed on the basis of the McClure model with allowance for the displacement of the Fermi level in a strong magnetic field; the dashed line is the theoretical variation of the extremal cross section with pressure. The black points represent the oscillation frequency in a strong magnetic field. b) Variation under pressure of the extremal cross sections of the ECES in $H\|C_1$ for the same alloy. The solid curves are theoretical curves computed on the basis of the McClure model.

ECES, such as is each of the three quasiellipsoids in Bi in the range of angles $\varphi = 30$—$90°$, can be approximated with a sufficient degree of accuracy by the angular dependence of the cross sections of a cylinder described
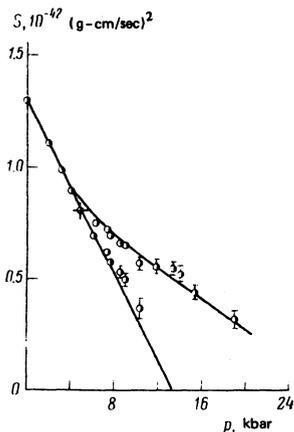

FIG. 2. Dependence on pressure p of the extremal cross sections of the ECES in Bi in $H\|C_1$. The solid curves are theoretical curves computed on the basis of the McClure model.
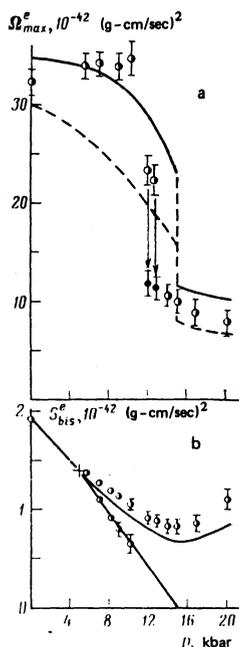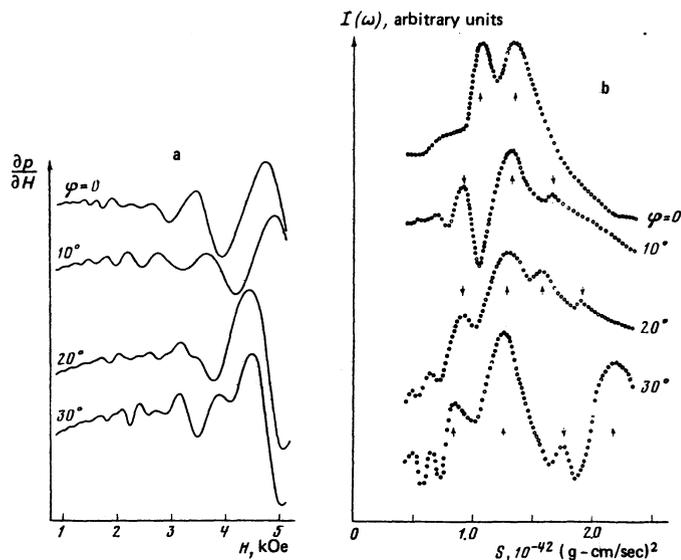

FIG. 4. a) Oscillations in $\partial\rho/\partial H$ in a Bi-Te alloy $(n_e = 4.9 \times 10^{17}\text{cm}^{-3})$ as the field H is rotated in the basal plane. The pressure $p = 8.4$ kbar. The angle φ is measured from the binary axis. b) The spectral densities, $I(\omega)$, of the indicated oscillations as calculated on a computer. Along the abscissa axis is plotted the cross section S, which is proportional to the oscillation frequency.
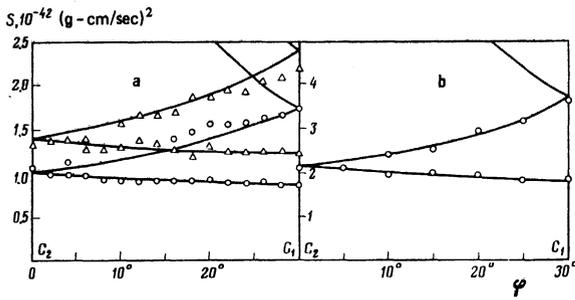
FIG. 5. Angular dependences of the extremal cross sections, S, of the ECES in a Bi-Te alloy ($n_g = 4.9 \times 10^{17}$cm^{-3}) at $p = 8.4$ kbar (a) and $p = 0$ (b). The solid lines are theoretical curves computed on the basis of the cylindrical ECES model.
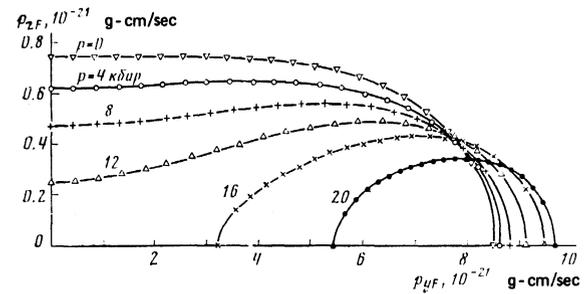

FIG. 6. The contours $p_z(p_y)$ of the ECES in the $p_x = 0$ plane ($p_x \parallel C_2$), computed on the basis of the McClure model at different pressures. The scale along the p_z axis is five times larger than the scale along the p_y axis.

around the ECES in such a way that the axis of the cylinder is parallel to the long axis of the ECES. The angular dependences of the ECES cross sections close to S_{min} are well approximated by the cross sections of three cylinders described around the quasiellipsoidal ECES only in the region of pressures $p \lesssim 5$ kbar and $p \gtrsim 13$ kbar. In the range $5 \lesssim p \lesssim 13$ kbar the $S(\varphi)$ and $S(p)$ curves look as if each of the three ECES were represented by two coaxial cylinders, the difference between the cross sections of these two cylinders being equal to zero at $p \sim 5$ kbar and increasing as the pressure is increased to $p_k \sim 13-15$ kbar, when the cross section of the smaller cylinder vanishes.

It should be noted that on the spectral-density curves (Fig. 4b) the contribution, $I(\omega_1)$, of the lower frequency ω_1 is always lower than the maximum of $I(\omega_2)$ ($\omega_1 < \omega_2 < \omega_3 < \omega_4$), the ratio $I(\omega_1)/I(\omega_2)$ decreasing as p is increased from ~ 5 to ~ 13 kbar. The pressure dependences of the oscillation frequencies (Fig. 2) and the $S(\varphi)$ curves at fixed pressures for pure Bi are completely similar to the corresponding dependences for the Bi-Te alloys (Figs. 4a and 5), although in the $\sim 5-13$ kbar pressure range the quantity $I(\omega_1)/I(\omega_2)$ has a smaller value in Bi than in the Bi-Te alloys.

The obtained pressure dependences of the cross sections and the angular dependences for $p = $ const can be interpreted in the following way. As p is increased the parameter $|\varepsilon_{gL}|$ increases: $\varepsilon_{gL} < 0$, $\varepsilon_{gL} = -|\varepsilon_{gL0}| - |\alpha| p$. For $p = 0$ there can be no saddle point in the spectrum when $\varepsilon_{gL} < 0$ [see (3)]. However, as $|\varepsilon_{gL}|$ increases, there first appears a saddle point at the bottom of the band ($Q_{22}^2/\alpha_v = \frac{1}{2}|\varepsilon_{gL}|$) and then a further increase in $|\varepsilon_{gL}|$ induces a change in the ECES, which, starting from $p \sim 5$ kbar (the cross in Figs. 2 and 3) and ending at $p \sim 13-15$ kbar, becomes dumbbell-like (Fig. 6).

From the dispersion equation (2) we can find the conditions under which the inequality $\partial k_x^2/\partial k_y^2 > 0$, which corresponds to the appearance of the dumbbell-shaped ECES

$$\tfrac{1}{2}\varepsilon_F(\alpha_v - \alpha_c) - \tfrac{1}{4}\varepsilon_{gL}(\alpha_v + \alpha_c) - Q_{22}^2 > 0 , \qquad (5)$$

is fulfilled. In this case when the field is oriented along the direction of elongation of the ECES there arises along with the minimum central cross section, $S_{bis\,1}$, of the "neck" of the dumbbell a second, somewhat larger, extremal cross section, $S_{bis\,2}$, of the "belly" of the

dumbbell. The cross section $S_{bis\,2}$ can be found by calculating from (2) the k_y dependence of S_{bis} and then, using the equation $\partial S_{bis}/\partial k_y = 0$, determine the k_y value, $k_{y\,extr}$, corresponding to the "belly" of the dumbbell:

$$S_{bis2} = \frac{\pi}{Q_{11}Q_{33}}\left[\left(\varepsilon_F - \frac{1}{2}\varepsilon_{gL} - \frac{1}{2}\alpha_c k_y^2\right)\left(\varepsilon_F + \frac{1}{2}\varepsilon_{gL} + \frac{1}{2}\alpha_v k_y^2\right) - Q_{22}^2 k_y^2\right]$$

for $\qquad\qquad\qquad\qquad\qquad\qquad\qquad\qquad\qquad (6)$

$$k_y^2 = k_{y\,extr}^2 = \frac{\varepsilon_F(\alpha_v - \alpha_c) - \tfrac{1}{2}\varepsilon_{gL}(\alpha_c + \alpha_v) - 2Q_{22}^2}{\alpha_c \alpha_v} . \qquad (7)$$

At a pressure $p_k = 13.5 \pm 0.8$ kbar in the case of Bi and $p_k \sim 15$ kbar in the case of the Bi-Te alloys (the difference in p_k is a consequence of the difference in ε_F), the cross section

$$S_{bis\,1} = \pi(\varepsilon_F^2 - \tfrac{1}{4}\varepsilon_{gL}^2)/Q_{11}Q_{33} \qquad (8)$$

degenerates into a point. At this moment

$$S_{bis2} = \frac{\pi\alpha_v}{Q_{11}Q_{33}\alpha_c}\left(\frac{1}{2}\varepsilon_{gL}(p = p_K) + \frac{Q_{22}^2}{\alpha_v}\right)^2 . \qquad (9)$$

At $p > p_k$ the ECES becomes a doubly connected surface (Fig. 6 and Fig. 12 below). The oscillations from the central cross sections ($k_y = 0$) disappear (Figs. 2 and 3) and only oscillations from the cross sections at $k_y = k_{y\,extr}$ are observed.

To the decrease of $I(\omega_1)/I(\omega_2)$ as p increases from ~ 5 to ~ 13 kbar corresponds the decrease of the radius of curvature in the region of the neck of the dumbbell (Fig. 6), as a result of which the contribution to the oscillations from the extremal orbit of the neck decreases. The angular dependences of the oscillation frequencies from the cross sections close to the minimal cross sections (Fig. 5) are well described by the following transformation of the ECES under pressure: up to $p \sim 5$ kbar each of the three ECES can be approximated by one circumscribed cylinder; in the range $5-13$ kbar, by one circumscribed cylinder touching the ECES in the region of the belly of the dumbbell and one inscribed cylinder touching the ECES in the region of the neck of the dumbbell. At $p > p_k$ the dependences $S(\varphi)$ for the six ECES that arise can again be approximated by the cross sections of three cylinders each of which is described around two drop-shaped ECES formed as a result of the rupture of one dumbbell.

In Figs. 2 and 3 the solid lines are theoretical curves

computed from the formulas (6)—(8) with the parameters

$$Q_{11}=0.435, \quad Q_{22}=0.015, \quad Q_{33}=0.327,$$
$$\alpha_c=1.3, \quad \alpha_v=1.53, \quad \varepsilon_{gL0}=-7 \text{ meV} . \tag{10}$$

Since $\varepsilon_{gL}(p) = \varepsilon_{gL0} + \alpha p$, we can determine $\varepsilon_F(p)$ from $\varepsilon_{gL}(p)$ found from (8). Simultaneously, ε_F was also computed from the equation $n=p$ (for Bi) or $n-p=n_0$ (for the Bi-Te alloys); here n_0 is the donor-electron concentration. The dependence of the T-hole concentration on pressure was computed from the minimal cross sections, $S_{min}^h(p)$, for Bi, which were taken from Refs. 22 and 23:

$$p = p_{Bi}(S_{min}^h(p)/S_{min\ Bi}^h)^{1/2}.$$

The $\varepsilon_F(p)$ values obtained by the two different methods coincided with each other to within ~0.8 meV. After the rupture of the neck of the dumbbell ($p > p_k$) only one cross section ($S_{bis\ 2}$) was observed in $H\|C_1$, and ε_F was determined by the second method.

Notice that the increase of the cross section $S_{bis\ 2}$ at high p in the Bi-Te alloys (Fig. 3) is due to the fact that these alloys differ from Bi in the character of the motion, as the pressure is increased, of the Fermi level, which at $p > p_k$, when there are already no holes at T, is established in such a way that the electron concentration satisfies the condition $n = n_0 = \text{const}$, which leads to the increase of ε_F and, consequently, to a limited increase in $S_{bis\ 2}$ as p increases.

In the calculation the quantity $\alpha \equiv \partial \varepsilon_{gL}/\partial p$ was found from the formula (9) for the cross section, $S_{bis\ 2}$, of the belly of the dumbbell at the moment of formation of the conic point ($p = p_k$) and was for the gap $\varepsilon_{gL} = -7$ meV at zero pressure equal to -2.9 meV/kbar, which is close to the value $\alpha = -(2.5 \pm 0.2)$ meV/kbar for the semiconducting alloys $Bi_{1-x}Sb_x$.[18] The cross-section calculations carried out on the basis of the McClure model with the parameter values taken from Ref. 38 yield results that agree with the experimental cruves just as well as the results obtained in the computation with the parameters given above in the present paper if we set $\partial \varepsilon_{gL}/\partial p = -3.3$ meV/kbar. It should be noted that the results of the computation with the use of the spectral parameters given by McClure in Ref. 12 disagree sharply with the experimental data: even for $\varepsilon_{gL0} = -13$ meV they yield the rate $\partial \varepsilon_{gL}/\partial p \sim -16$ meV/kbar, which is many times greater than the experimental value of $-(2.5 \pm 0.2)$ meV/kbar.

THE PRESSURE DEPENDENCE OF THE OSCILLATION FREQUENCY FROM THE LARGE CROSS SECTIONS

Doping with Te is convenient in that, first, as indicated above, it leads to the increase of the amplitude and the number of oscillations from the large ECES cross sections[26] and, secondly, it increases the difference between the maximum cross section, S_{max}^h, of the hole FS and the maximum cross section, S_{max}^e, of the ECES. (In pure Bi these cross sections are close, having in units of 10^{-42}g-cm^2/sec the values $S_{max}^e = 19.27$, $S_{max}^h = 22.5$.[6]) Therefore, for $H\|C_2$ the oscillation curves in
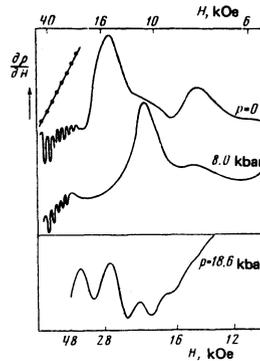

FIG. 7. Oscillations in $\partial \rho/\partial H = f(1/H)$ in a Bi-Te alloy ($n_e = 4.9 \times 10^{17}$cm^{-3}) for $H\|C_2$. On the left above is demonstrated the determination of the period of the oscillations from the dependence of the arbitrary quantum number of the oscillation on $1/H$.

strong fields for the Bi-Te alloys, in contrast to the curves for Bi, are due only to the oscillations from the S_{max}^e, and do not represent a superposition of close frequencies from S_{max}^e and S_{max}^h (Fig. 7).

Under pressure the frequency, Ω_{max}^e, of the oscillations from S_{max}^e initially ($0 \lesssim p \lesssim 11$ kbar) increases slightly, or remains almost constant (Figs. 3 and 8). In this case the $\partial \rho/\partial H = f(1/H)$ curves have a monochromatic composition. In the range 12 kbar $\lesssim p \lesssim 14$ kbar the character of the oscillation curves changes: in fields of intensity higher than 30 kOe the fundamental frequency disappears, and there appears a frequency lower than the fundamental frequency by roughly a factor of two (Fig. 9). Upon further increase of the pressure the frequency Ω_{max}^e at first ($p = 13 - 15$ kbar) decreases sharply (roughly by a factor of two) and then decreases more slowly with increasing pressure. For all the investigated Bi-Te alloys the oscillations from S_{max}^e depend on pressure in like manner. In the case of pure Bi we investigated only the initial part of the Ω_{max}^e (p) curve for pressures $p < 5$ kbar: the S_{max}^e oscillations disappeared at $p \gtrsim 5$ kbar. In the range 0—5 kbar the frequency, Ω_{max}^e, of the oscillations in Bi remained roughly constant. The absence of oscillations in Bi at $p \gtrsim$ kbar can, apparently, be explained by the fact that the
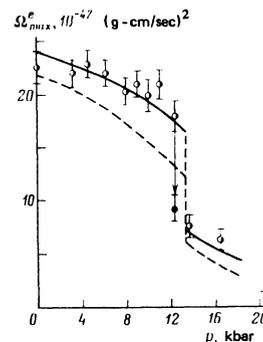

FIG. 8. Pressure dependence of the oscillation frequency on the maximal cross section of the ECES in a Bi-Te alloy ($n_e = 3.2 \times 10^{17}$cm^{-3}). The solid and dashed curves are respectively theoretical oscillation-frequency and extremal-cross-section curves computed on the basis of the McClure model.
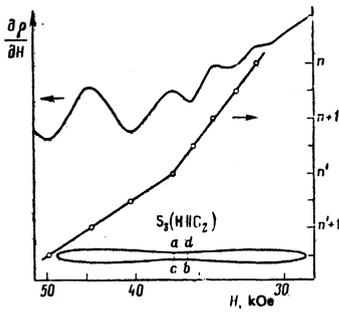
FIG. 9. The halving of the oscillation frequency as a result of the magnetic-field-induced change in the connectivity of the ECES. The dumbbell-like contour is the theoretical dependence of p_z on p_y in the $p_x = 0$ plane at $p = 12.2$ kbar as derived from the McClure model.

single-crystal samples of pure Bi were more plastic than the Bi-Te alloy samples, as a result of which the presence of some nonhydrostatic pressure component in the pressure-booster channel led to partial damage of the sample, which affected primarily the oscillations from the large cross sections.

In analyzing the $\Omega^e_{max}(p)$ dependence it is necessary to take into account the fact that in the case of the $H \| C_2$ field orientation, starting from some value of H, the light carriers on two ECES are in the ultraquantum limit (see Fig. 7, where the extremum corresponding to the light-electron yield of the Landau level 0^+ can be seen), i.e., there remains under the Fermi level in each of these ECES a single Landau cylinder whose capacity, $n_{1,2}$, is proportional to the magnetic field:

$$n_1 = n_2 = 2eHp_x / (2\pi\hbar)^2 c,$$

where p_x is the maximum momentum of the light electrons in the direction of the field H. The equality of the electron and hole concentrations leads to a situation in which an increase in the magnetic-field intensity leads to the overflow of carriers from the third ECES and from the hole FS into levels lying in the ultraquantum limit,[32] in consequence of which the Fermi level moves downward counter to the motion of the Landau levels in the unquantized ECES. As a result, the oscillation frequency is no longer connected through the relation $S_{extr} = e\hbar\omega_{osc}/c$ with the corresponding extremal cross section S_{extr}, and the computation of S_{extr} from ω_{osc} yields too high an S_{extr} value.

In view of this it was of interest to measure the cross section, $S(H \| C_3)$, that is close to the intermediate cross section, S_{int}, of the ECES for a field orientation along the trigonal axis C_3, when the cross sections of all the three ECES are equal and there is virtually no overflow of carriers in fields of up to 60 kOe. To determine $S(H \| C_3)$ as a function of p in Bi we measured the angular dependences of the oscillations $\partial\rho/\partial H$ as the field was rotated in the bisectrix-trigonal plane for different p (Fig. 10). The application of transverse magnetic-field modulation allowed us to separate out near C_3 only the oscillations from the electronic cross sections, since in this angle range the extremal cross section of the hole FS weakly depends on the angle. The cross sections
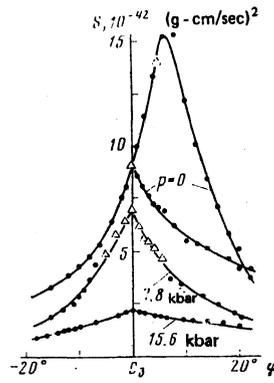

FIG. 10. Angular dependences of the extremal ECES cross sections in Bi when the field is rotated in the bisectrix-trigonal plane. The points $\triangle$ indicate the extremal cross sections as determined from the second harmonic of the oscillations.

near the trigonal axis were determined from the halved frequency of the second harmonic of the oscillations, since a strong second harmonic of the oscillations was observed in such a field orientation because of the closeness of the spin-damping angle ($H \| C_3$). The cross sections S ($H \| C_3$) determined from the angular dependences at different pressures are shown in Fig. 11. The cross section S ($H \| C_3$) decreases monotonically with pressure in the region of pressures $p \lesssim 13$ kbar, sharply (roughly by a factor of two) in the range 13–14.5 kbar, and again monotonically thereafter. It is worth noting that spin damping of the fundamental harmonic of the oscillations was no longer observed near the trigonal axis at two pressures after the drop in the $S(p)$ curve: 14.5 and 15.6 kbar (Fig. 10).

The different behaviors of the cross sections $S(H \| C_3)$ (Fig. 11) and the frequencies $\Omega^e_{max}(p)$ (Fig. 3) as functions of the pressure indicates that the increase of the frequency Ω^e_{max} in the region $p \lesssim 11$ kbar is not accompanied by an increase in the corresponding maximum cross section S^e_{max}, but is the result of the growth with pressure of the corrections for the motion of the Fermi level. The correction for the variation of ε_F with the field H, a correction which characterizes the difference between the true extremal cross section and the "cross section" computed from the frequency, ω_{osc}, of the oscillations produced in the case of a moving ε_F, increases upon doping with Te and under the action of pressure,
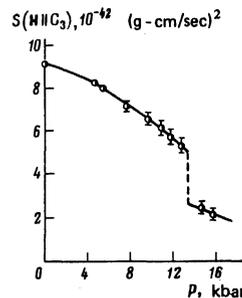

FIG. 11. The extremal ECES cross sections, $S(H \| C_3)$, in Bi when the field is oriented along the trigonal axis (C_3) as functions of the pressure p.

since in both cases the density of states of the holes at T decreases; these holes, by overflowing into the electronic valleys found in the ultraquantum limit, slow down the Fermi level.[1]

The decreasing part of the $\Omega_{max}^e(p)$ curves for the Bi-Te alloys, as well as the change by a factor of two of the cross section $S(H||C_3)$ in Bi, occurs in the pressure range 12-15 kbar, i.e., just at those pressures at which the cross section of the neck of the dumbbell vanishes, and to the change in $\Omega_{max}(p)$ and the halving of S $(H||C_3)$ corresponds the rupture of the dumbbell-like ECES into two at $p = p_k$.

MAGNETIC-FIELD-INDUCED CHANGES IN THE CONNECTIVITY OF THE ECES

In the pressure range 12-14 kbar, as described above, the oscillation frequency in fields of intensity up to ~35 kOe is roughly twice the oscillation frequency in $H \gtrsim 35$ kOe (Fig. 9). Such a distinctive feature is observed in all Bi-Te samples in the indicated pressure range. Notice that the pressures of 12-14 kbar precede the transition from a dumbbell-like to a doubly-connected ECES, i.e., the cross section of the neck of the dumbbell is already sufficiently small. A similar situation obtains in Te, whose valence band is described by a dispersion law with a saddle point. At a definite hole concentration in Te the Fermi level ε_F passes near the saddle point ε_k and an intraband magnetic breakdown is observed in strong fields.[34] The intensity, H_b, of the field in which a breakdown occurs between the close trajectories ad and bc (Fig. 9) can be estimated from the formula

$$H_b \sim \Delta\varepsilon/\mu_0, \tag{11}$$

where $\Delta\varepsilon = |\varepsilon_F - \varepsilon_k|$ and μ_0 is the Bohr magneton. For $H_b \sim 35$ kOe the estimate from (11) yields $\Delta\varepsilon \sim 0.4$ meV.

In the case of the Bi-Te alloys with the field orientation $H||C_2$ we should, besides the intraband magnetic breakdown, also take into account the displacement of the Fermi level ε_F in the magnetic field as a result of overflowing. Estimates show that because of the overflowing ε_F gets shifted by ~4 meV in fields of intensity 30-60 kOe. The downward motion of ε_F along the conduction band leads to a situation in which at first the condition, (11), for magnetic breakdown begins to be fulfilled, then ε_F coincides with ε_k and a change in the connectivity of the ECES occurs. Further displacement of the Fermi level, in this case from the saddle point ε_k, will violate the condition, (11), for the occurrence of a magnetic breakdown. However, the oscillation frequency will remain half as high, since the ECES is doubly connected when $\varepsilon_F < \varepsilon_k$.

Therefore, the reduction of the oscillation frequency by a factor of two in fields of intensity $H \gtrsim 35$ kOe is both a consequence of the intraband magnetic breakdown and a result of the change in the connectivity of the ECES upon the displacement of the Fermi level in the magnetic field as a result of the overflow effect. These effects cannot be divorced from each other in this case.

THE RECONSTRUCTION OF THE SPECTRUM OF Bi UNDER PRESSURE

It follows from the results of Refs. 20 and 35 that in the region of hole Fermi energies ε_F^h less than ε_F in Bi (10.9 meV[36]) the energy spectrum of the holes at T is described by Kane's two-band model with a gap $\varepsilon_{gT} = 200 \pm 40$ meV. According to this model, the decrease of the minimal cross section, S_{min}^h, of the hole ellipsoid under pressure[22,23] should be accompanied by a similar change in the large cross section S_{max}^h, i.e., the hole ellipsoid remains similar to itself when compressed.

The pressure dependences of the ECES cross sections, the angular dependences $S(\varphi)$ for fixed pressures, and the magnetic-field-induced change in the connectivity of the ECES in the pressure region where the cross section of the neck is small are in satisfactory agreement with the results obtained in a McClure-model calculation with the above-indicated [see (10)] values for the model parameters if we assume that the spectrum in Bi is inverted ($\varepsilon_{gL} < 0$) and the gap parameter $|\varepsilon_{gL}|$ increases with pressure at a rate of 2.9 meV/kbar. The obtained experimental data on the transition of the ECES in Bi at $p \sim 5$ kbar to a dumbbell-shaped ECES and on the rupture of the neck of the dumbbell at $p = 13.5 \pm 0.8$ kbar indicate that the model-parameter values given by McClure in Ref. 12 are too high. Using the reasonable—in our opinion—assumption that the value of the rate $\partial\varepsilon_{gL}/\partial p$ in Bi is close to the values in the alloys $Bi_{1-x}Sb_x$ (for $x \sim 8-10$ at. %), we can find that the parameters Q_{22} and α_v should satisfy the inequality

$$Q_{22}^2/\alpha_v < 0.0005 \text{ a.u. },$$

Notice also that the set of parameters (10) only satisfactorily describes both Édel'man's data for Bi at $p = 0$[36] and the various pressure dependences obtained in the present work.
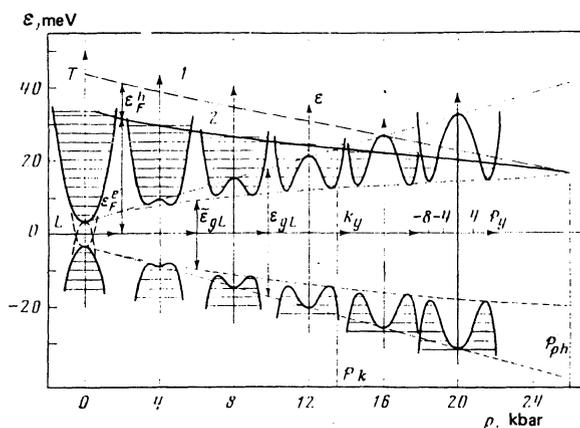
FIG. 12. Schematic representation of the reconstruction of the spectrum of Bi under pressure. The dependences of the electron and hole energy, ϵ, at L on the wave vector k_y at different pressures were computed on the basis of the McClure model. The dashed curve at $p = 0$ depicts the dependence of ϵ on k_y for $Q_{22} = 0$ (the AF model). The curves 1 and 2 respectively depict the motion under pressure of the T term and the Fermi level. The pressure p_k corresponds to the passage of the Fermi level through a saddle point, while the pressure p_{ph} corresponds to the metal-dielectric phase transition. The p_y values are given in units of 10^{-21} g-cm/sec.

The reconstruction scheme for the spectrum of Bi under pressure is shown in Fig. 12. The linear dependence of S_{min}^h on p presupposes the linear decrease of $\varepsilon(T) - \varepsilon_F \equiv \varepsilon_F^h$ under pressure and the vanishing of ε_F^h at $p = p_{ph} \sim 26$ kbar, when the ECES and the hole FS in Bi shrink to points.[37] For the parameters $Q_{22} = 0.015$ and $\alpha_v = 1.53$ the saddle point in the electron spectrum in Bi at $p = 0$ ($\varepsilon_{gL} = -7$ meV) is absent and appears only at $\varepsilon_{gL} = -8$ meV. The invertedness of the spectrum ($\varepsilon_{gL} < 0$) for $p = 0$ manifests itself only in some flattening of the extrema of the bands at L. When $|\varepsilon_{gL}|$ is increased, the bottom of the band flattens out even more and, starting from some pressure

$$p_s{}^e = \frac{1}{\alpha}\left(\frac{2Q_{22}{}^2}{\alpha_v}\right), \qquad p_s{}^h = \frac{1}{\alpha}\left(\frac{2Q_{22}{}^2}{\alpha_c}\right), \qquad (12)$$

a saddle point appears in the electron and hole spectrum at L. The T_{4S} term moves relative to the middle of the gap ε_{gL} with velocity $\beta = \partial\varepsilon_b/\partial p = 0.9$ meV/kbar (Fig. 12). The rupture of each of the three dumbbell-like ECES into two drop-like surfaces occurs at $p = p_k$, when the Fermi level ε_F passes through the saddle point, i.e., when $\varepsilon_F = -\frac{1}{2}\varepsilon_{gL}$.

The metal-dielectric phase transition at $p \sim 26$ kbar occurs through the shrinking of the six ECES to points and not through the shrinking of the three quasiellipsoidal ECES in Bi, as was thought earlier. At the transition point the Fermi level passes through the two minima forming the bottom of the conduction band. The points $\pm k_{y0}$ corresponding to these minima are determined from the condition $\partial\varepsilon(k_y)/\partial k_y = 0$:

$$(k_{y0}{}^2)_{1,2} = \left\{-4Q_{22}{}^2 - \varepsilon_{gL}(\alpha_c + \alpha_v) \pm 2Q_{22}|\alpha_c - \alpha_v|\right.$$

$$\times \left[\frac{1}{\alpha_c\alpha_v}\left(-Q_{22}{}^2 - \frac{1}{2}\varepsilon_{gL}(\alpha_c + \alpha_v)\right)\right]^{1/2}\left\}\left[2\alpha_c\alpha_v + \frac{1}{2}(\alpha_c - \alpha_v)^2\right]^{-1}. \quad (13)$$

The signs $\pm$ in front of the term $2Q_{22}$... determine the locations of the maxima and minima in the hole and electron bands at L. If $\alpha_c = \alpha_v$, then the terms are symmetric and the distance between the minima of the conduction band and the maxima of the valence band is equal to

$$\tilde\varepsilon_{gL} = 2\left[\frac{Q_{22}{}^2}{\alpha_{c,v}}\left(|\varepsilon_{gL}| - \frac{Q_{22}{}^2}{\alpha_{c,v}}\right)\right]^{1/2}. \quad (14)$$

The gap $\tilde\varepsilon_{gL}$, after the appearance of the saddle points in the spectrum, differs from the quantity $\varepsilon_{gL} \equiv \varepsilon(L_a) - \varepsilon(L_S)$.

It was observed in the investigation of the $Bi_{1-x}Sb_x$ alloys in the semiconductor region of compositions under pressure[18] that the 1.5 ± 0.2 meV/kbar rate of change of the direct gap after the inversion point is lower than the rate, $\alpha = 2.5 \pm 0.2$ meV/kbar, of change of the gap $\varepsilon_{gL} > 0$ up to the inversion pressure p_{inv}. This result is in accord with the appearance of saddle points in the spectrum, as a result of which the energy gap $\tilde\varepsilon_{gL}$ between the minima of the conduction band and the maxima of the valence band at the points $\pm k_{k0}$, (13), becomes smaller than the quantity $|\varepsilon_{gL}| = |\varepsilon(L_a) - \varepsilon(L_S)|$ [see (14)]. If we use the Q_{22}- and α_v-parameter values given in Ref. 12 for the $Bi_{1-x}Sb_x$ alloys, then the appearance of the saddle point should occur at pressures that exceed the inversion pressure by $\Delta p \approx 13$ kbar. How-

ever, experimentally, the post-p_{inv} rate of change of the gap, which is different from the preinversion rate, is observable even in the range $\Delta p = p - p_{inv} \sim 3$ kbar, which also indicates a value for Q_{22}^2/α_v substantially lower than the value given in Ref. 12.

In conclusion, we take the opportunity to express our sincere gratitude to S. D. Beneslavskiĭ and Ya. G. Ponomarev for useful discussions and to P. A. Saltykov for his help in the measurements.

[1]L. A. Fal'kovskiĭ, Usp. Fiz. Nauk 94, 3 (1968) [Sov. Phys. Usp. 11, 1 (1968)].

[2]V. S. Édel'man, Adv. Phys. 25, 555 (1976).

[2a]V. S. Édel'man, Usp. Fiz. Nauk 123, 257 (1977).

[3]B. Lax, J. G. Mavroides, H. J. Zeiger, and R. J. Keyes, Phys. Rev. Lett. 5, 241 (1960).

[4]A. A. Abrikosov and L. A. Fal'kovskiĭ, Zh. Eksp. Teor. Fiz. 43, 1089 (1962) [Sov. Phys. JETP 16, 769 (1963)].

[5]A. A. Abrikosov, J. Low Temp. Phys. 8, 315 (1972).

[6]V. S. Édel'man, Zh. Eksp. Teor. Fiz. 64, 1734 (1973) [Sov. Phys. JETP 37, 875 (1973)].

[7]V. S. Édel'man and M. S. Khaĭkin, Zh. Eksp. Teor. Fiz. 49, 107 (1965) [Sov. Phys. JETP 22, 77 (1966)].

[8]R. J. Dinger and A. W. Lawson, Phys. Rev. B7, 5215 (1973).

[9]R. N. Bhargava, Phys. Rev. 156, 785 (1967).

[10]S. Takaoka, H. Kawamura, K. Murase, and S. Takano, Phys. Rev. B13, 1428 (1976).

[11]B. A. Akimov, Candidate's Dissertation, Moscow State Univ., 1975.

[12]J. W. McClure, J. Low Temp. Phys. 25, 527 (1976); J. W. McClure and K. H. Choi, Solid State Commun. 21, 1015 (1977).

[13]L. G. Fereira, J. Phys. Chem. Solids 28, 1891 (1967).

[14]S. Golin, Phys. Rev. 166, 643 (1968).

[15]M. Maltz and M. S. Dresselhaus, Phys. Rev. B2, 2877 (1970).

[16]M. P. Vecchi and M. S. Dresselhaus, Phys. Rev. B9, 3257 (1974); B10, 771 (1974).

[17]M. H. Cohen, Phys. Rev. 121, 327 (1961).

[18]N. B. Brandt, S. M. Chudinov, and V. G. Karavaev, Zh. Eksp. Teor. Fiz. 70, 2298 (1976) [Sov. Phys. JETP 43, 1198 (1976)].

[19]N. B. Brandt, V. A. Yastrebova, and Ya. G. Ponomarev, Fiz. Tverd. Tela (Leningrad) 16, 102 (1974) [Sov. Phys. Solid State 16, 59 (1975)].

[20]N. B. Brandt, R. Müller, and Ya. G. Ponomarev, Zh. Eksp. Teor. Fiz. 71, 2268 (1976) [Sov. Phys. JETP 44, 1196 (1976)].

[21]E. S. Itskevich, I. P. Krechetova, and L. M. Fisher, Zh. Eksp. Teor. Fiz. 52, 66 (1967) [Sov. Phys. JETP 25, 41 (1976)].

[22]E. S. Itskevich and L. M. Fisher, Zh. Eksp. Teor. Fiz. 53, 98, 1885 (1967) [Sov. Phys. JETP 26, 66 (1968)].

[23]N. B. Brandt, Yu. P. Gaĭdukov, E. S. Itskevich, and N. Ya. Minina, Zh. Eksp. Teor. Fiz. 47, 455 (1964) [Sov. Phys. JETP 20, 301 (1965)].

[24]N. B. Brandt, N. Ya. Minina, and Yu. A. Pospelov, Fiz. Tverd. Tela (Leningrad) 10, 1268 (1968) [Sov. Phys. Solid State 10, 1011 (1968)].

[25]N. B. Brandt and N. I. Ginzburg, Zh. Eksp. Teor. Fiz. 39, 1554 (1960) [Sov. Phys. JETP 12, 1082 (1961)].

[26]V. V. Moshchalkov and G. A. Mironova, Pis'ma Zh. Eksp.

Teor. Fiz. **26**, 538 (1977).

[27]E. S. Itskevich, Prib. Tekh. Eksp. No. 4, 148 (1963); N. B. Brandt and Ya. G. Ponomarev, Zh. Eksp. Teor. Fiz. **55**, 1215 (1968) [Sov. Phys. JETP **28**, 635 (1969)].

[28]N. E. Alekseevskiĭ, N. B. Brandt, and T. I. Kostina, Izv. Akad. Nauk SSSR Ser. Fiz. **16**, 233 (1952).

[29]B. A. Akimov, V. V. Moshchalkov, and S. M. Chudinov, Fiz. Nizk. Temp. **4**, 60 (1978).

[30]G. A. Antcliffe and R. T. Bate, Phys. Rev. **160**, 531 (1967).

[31]P. Cucka and C. S. Barrett, Acta Crystallogr. **15**, 865 (1962).

[32]G. E. Smith, G. A. Baraff, and J. M. Rowell, Phys. Rev. **135**, A1118 (1964).

[33]N. B. Brandt, V. V. Moshchalkov, and S. M. Chudinov, Pis'ma Zh. Eksp. Teor. Fiz. **25**, 361 (1977) [JETP Lett.

25, 336 (1977)].

[34]Yu. V. Kosichkin, Kand. dissertatsiya (Candidate's Dissertation), FIAN, Moscow, 1970; V. B. Anzin, M. S. Bresler, I. I. Farbshtein, Yu. V. Kosichkin, and V. G. Veselago, Phys. Status Solidi **40**, 417 (1970).

[35]R. T. Bate and N. G. Einspruch, Phys. Rev. **153**, 796 (1967).

[36]V. S. Edel'man, Dokt. dissertatsiya (Doctor's Dissertation), IFP, Moscow, 1975.

[37]D. Balla and N. B. Brandt, Zh. Eksp. Teor. Fiz. **47**, 1653 (1964) [Sov. Phys. JETP **20**, 1111 (1965)].

[38]E. P. Buyanova, V. V. Evseev, G. A. Mironova, G. A. Ivanov, and Ya. G. Ponomarev, Fiz. Tverd. Tela (Leningrad) No. 8 (1978).

Translated by A. K. Agyei

Contribution to the theory of defectons in quantum crystals

D. Pushkarov and Z. Koĭnov

Solid State Physics Institute, Bulgarian Academy of Sciences
(Submitted 2 December 1977)
Zh. Eksp. Teor. Fiz. **74**, 1845–1852 (May 1978)

Deformation produced in a quantum crystal by the presence of a point defect is considered. It is shown that a bound defecton state with deformation of the lattice can be produced in the one-dimensional case. It is shown that the deformation moves together with the defect with constant velocity without changing shape. In the three-dimensional case, the bound state is produced at deformation dimensions for which the continual approximation can be used.

As shown by Andreev and I. Lifshitz,[1] at low temperatures point defects in quantum crystals are transformed into quasiparticles — defectons. A quantum theory of defectons, based on a microscopic model, was constructed by one of us.[2] Defectons connected with motion of complexes of defects were considered by Andreev and Meĭerovich.[3,4] They have also shown that even in a three-dimensional crystal there can exist defectons with one or two degrees of freedom. In these papers the lattice deformation around the defect was assumed specified, and its influence on the defecton spectrum was taken into account. A one-dimensional model of a quantum crystal with a defect was considered in,[5] where it was shown that a self-consistent state can be produced, such that the defect moves together with the deformation it produces. The appearance of this state is mathematically connected with the soliton solutions of the nonlinear Schrödinger equation. In the approximation used in,[5] no account was taken of the change of the probability of a transit of a defect to a neighboring node as a result of lattice deformation.

In this paper we consider both a one-dimensional and a three-dimensional crystal with a defect. In the harmonic approximation, the system Hamiltonian can be written in the form

$$\hat{H} = \sum_{R,\alpha} \frac{m}{2} (\dot{\xi}_R^\alpha)^2 (1 + \mu B_R^+ B_R) + \frac{1}{2} \sum_{RR'\alpha\beta} L_{R-R'}^{\alpha\beta} \xi_R^\alpha \xi_{R'}^\beta + \frac{1}{2} \sum_R \Lambda_R B_R^+ B_R - \frac{1}{2} \sum_{RR'} A_{R-R'} B_R^+ B_R,$$ (1)

where ξ_R^α is the α component of the displacement vector of the atom situated at the site R compared with its equilibrium position in a perfect crystal; $\mu = (M-m)/m$, where M and m are respectively the masses of the impurity and of the host lattice atom;

$$\Lambda_R = \sum_{R'} \Lambda_{RR'}(\xi_R - \xi_{R'})$$ (2)

is the difference between the interaction energy of the defect with the remaining atoms, and the interaction energy of the host atom with them. The second sum in (1) describes the potential energy of an ideal crystal in the harmonic approximation; B_R^+ and B_R are the Bose operators of defect creation and annihilation at the site R; $A_{R-R'}$ is the amplitude of the probability of the transfer of a defect from site R to site R'.

The solution of the Schrödinger equation

$$i\hbar\partial\Psi/\partial t = \hat{H}\Psi$$ (3)

will be sought in the form of an expansion

$$\Psi = \sum_R a_R(t) \Psi_R,$$ (4)

where $\Psi_R = B_R^+|0\rangle$ is the wave function of the system with a defect localized at the site R; $|0\rangle$ is the wave function of the ideal crystal. Naturally, the coefficients a_R should satisfy the normalization condition

$$\sum_R |a_R|^2 = 1.$$ (5)